CRITICAL EVALUATION OF THE PULSED LASER METHOD FOR SINGLE EVENT EFFECTS TESTING AND FUNDAMENTAL STUDIES

J.S. Melinger, S. Buchner, D. McMorrow, W.J. Stapor, T.R. Weatherford, and A.B. Campbell
Naval Research Laboratory, Code 6613, Washington DC 20375

H. Eisen
Army Research Laboratory, 2800 Powder Mill Road, Adelphi MD 20783

Abstract

In this paper we present an evaluation of the pulsed laser as a technique for single events effects (SEE) testing. We explore in detail the important optical effects, such as laser beam propagation, surface reflection, and linear and nonlinear absorption, which determine the nature of laser-generated charge tracks in semiconductor materials. While there are differences in the structure of laser- and ion-generated charge tracks, we show that in many cases the pulsed laser remains an invaluable tool for SEE testing. Indeed, for several SEE applications, we show that the pulsed laser method represents a more practical approach than conventional accelerator-based methods.

I. INTRODUCTION

Particle accelerator testing is the standard method used to characterize the sensitivity of modern device technology to single event effects (SEE). However, because accelerator testing is often both expensive and not easily accessible, and, to date, has provided only limited spatial and temporal information, other techniques that do not suffer from these limitations are needed. The pulsed (sub-nanosecond) laser is one such technique that has generated much interest in the SEE community. For example, the past few years have seen the pulsed laser used successfully to characterize SEE behavior in both memories and logic circuits [1-3], and, also, as a tool to understand fundamental charge collection mechanisms in semiconductor devices [4]. Yet, despite the significant advances made in the development of the pulsed laser technique, there still remain important questions regarding the ability of the laser to simulate ion-induced SEE.

An important point to keep in perspective is that neither accelerators nor pulsed lasers reproduce all aspects of space particle radiation and, as such, both forms of testing represent an approximation to the space environment. Nevertheless, our goal remains to understand and predict the performance and reliability of integrated circuits in various space environments. A thorough understanding of the strengths and weaknesses of each method of simulation is crucial.

Our goal is to examine the pertinent physics involved in the pulsed laser technique in order to improve potential users' understanding as to what information can be obtained that is a direct simulation of space-particle effects. We comment on previous questions raised in the SEE community regarding the use of laser generated charge tracks in semiconductors as an approximation to that generated by an ion-strike, and, in particular, clear up some misconceptions about the laser technique which have appeared recently [5]. Finally, we illustrate how the laser technique provides complimentary information to that obtained from accelerator testing, with some unique characteristics and capabilities that give rise to some distinct advantages over accelerator methods.

The paper is arranged as follows. Initially, we address the optical considerations that lead to the generation of a charge track produced by a focused laser pulse. We discuss in detail the role played by nonlinear absorption, and stress the importance of choosing a proper working wavelength so that nonlinear absorption effects, and other uncertainties related to the light-matter interaction, can be minimized. We then discuss the mechanisms that lead to charge collection from both laser- and ion-generated charge tracks. We present both experimental and theoretical evidence which supports our previous assertion that for many laboratory simulations of space particle effects, laser excitation provides a reasonable approximation to an ion strike. Finally, we point out inherent advantages and disadvantages of laser testing as compared to ion testing, and assess the two techniques based upon their respective feasibility of application to specific SEE testing situations.

II. CHARGE GENERATION BY LASER PULSES: OPTICAL EFFECTS

A. Laser Charge Tracks

In performing laser-based SEE measurements it is important for the experimentalist to work in a regime where the maximum intensity of the laser pulse is sufficiently small so that linear optics adequately describes the light-matter interaction. In the linear regime, both laser beam propagation and loss are adequately described by the material's linear susceptibility. Importantly, in the linear regime, complete knowledge of parameters such as laser spot size (focus) and material absorption is readily determined from the well-known (linear) refractive index, n, and linear absorption coefficient, α.

The most widely encountered laser beam is one where the radial intensity distribution is Gaussian. The propagation

U.S. Government Work Not Protected by U.S. Copyright

of Gaussian beams in linear media may be derived from the wave equation [6]. The longitudinal profile of a laser beam propagating through a model silicon device is shown in Fig. 1. Here, the beam radius, $\omega(z)$ (the point at which the laser intensity decays to 1/e of its value on axis), is given by [6]:

$$\omega^2(z) = \omega_o^2\left[1+\left(\frac{\lambda z}{\pi\omega_o^2 n}\right)^2\right], \tag{1}$$

where z is the propagation distance into the medium, ω_o is the 1/e radius of the laser spot at the surface (focus), and λ is the wavelength. There are two parameters shown in Fig. 1 which are important to SEE measurements. The first is the confocal length,

$$z_o = \pi n\frac{\omega_o^2}{\lambda}, \tag{2}$$

which represents the penetration length at which the beam diameter has expanded to $\sqrt{2}$ times its value at the focus. The second is the laser spot diameter, $2\omega_o$, which is determined by the optical focusing apparatus, and is written as

$$\omega_o = \frac{4f\lambda}{\pi D}, \tag{3}$$

where f is the focal length of the lens used to focus the laser beam, and D is the diameter of the laser spot illuminated on the lens. Fig. 1 clearly shows that the wavefront does not form a cone with an infinitely sharp point at the focus. The wavefront at the focus is parallel to the semiconductor surface, and the wave-vector is normal to the surface. Both of these conditions are readily achieved in the laboratory. This is an important point as previous discussions of the pulsed laser technique [5] have assumed a "cone" of incident rays, which is both unphysical and predicts an erroneously large surface reflection. Fig. 1 also illustrates how the laser beam diameter diverges as the beam penetrates into the device. This implies that the charge density (neglecting absorption) decreases by a factor of 2 at a penetration depth equal to the confocal length. For silicon, assuming a laser spot diameter at the surface of $\approx$ 1 μm and a wavelength of 0.80 μm (which are typical experimental values), the confocal length is about 3.6 μm (compare with $z_o \approx 1$ μm in air).

In the linear regime, material absorption is described by Beer's law which is expressed as

$$I(z) = I_o \exp(-\alpha z), \tag{4}$$

where I_o is the intensity entering the absorbing material, and α is the linear absorption coefficient [for simplicity here and in the equations below, both the temporal and radial dependencies of the intensity have been suppressed]. Eqs. 2 and 4 indicate that both material absorption and spreading of the beam lead to a reduction in the charge density created by a laser pulse as it propagates into the device. In contrast,

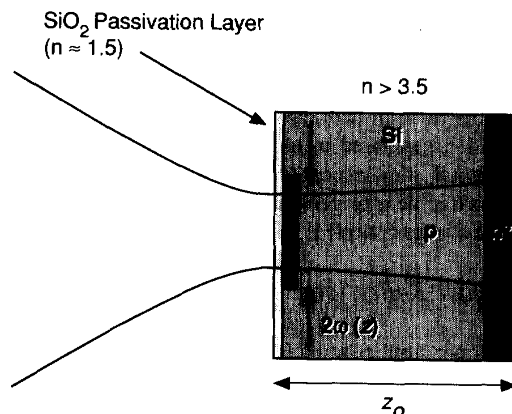

Figure 1. Longitudinal laser beam propagation in a model silicon device. The drawing shows how the beam wavefront at the surface is parallel at the focus. The high refractive index of silicon (n ≈ 3.5 at λ = 0.80 μ) keeps the beam from diverging as rapidly as in air. ω_o is the 1/e radius of the beam, and z_o is the confocal length which is the distance over which the transverse beam profile doubles in area.

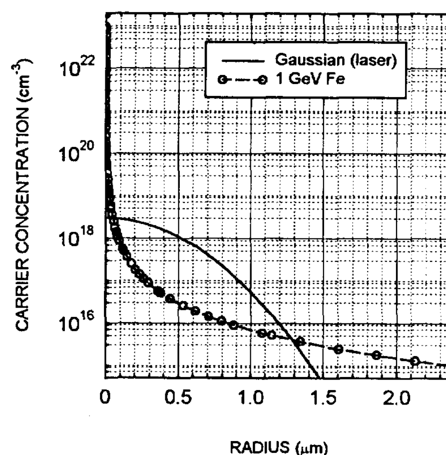

Figure 2. Radial charge density profile generated by a 1-GeV Fe ion and by a pulsed laser beam at a distance of 0.125 μm below the surface. The incident LET of the ion and the laser are the same.

compared to a laser pulse, a high penetration-depth ion generates a relatively constant charge density. As an example, Fig. 2 compares the radial charge density profile at a depth of 0.125 μm for a 1-GeV Fe ion as calculated by TRKRAD [7], and that from a Gaussian profile laser pulse with the same effective stopping power, or linear energy transfer (LET). Clearly, the ion produces a much more highly peaked radial charge distribution than the laser. The different radial charge distribution generated by the laser compared to the ion is of fundamental importance to SEE measurements, since the lower charge density generated by the laser track can affect the total charge collected.

B. Surface Reflections

Proper application of the laser technique requires an accurate knowledge of the amount of light that enters the device, since the number of photons is directly related to the charge generated. The amount of light entering a device will depend on the nature of the device surface, and on the presence of passivation layers used to protect the semiconductor surface. For example, if the interfaces which bound the passivation layer (see Fig. 3) are flat across the laser spot, then the passivation layer in effect acts as a Fabry-Perot etalon. To gain a measure of how the transmission of light into the device depends on the surface characteristics, we analyze a representative case illustrated in Fig. 3, which depicts a silicon substrate covered by a layer of silicon dioxide (SiO_2). The transmission of light into the silicon substrate may be calculated from the formula [8]

$$I_T = I_o\left[\frac{T^2}{1-R^2}\right]\left[\frac{1}{1+F\sin^2(\Delta/2)}\right], \tag{5}$$

where I_T is the intensity transmitted to the silicon substrate, and I_o is the intensity incident at the passivation layer. Also,

$$T = t_1 t_2 \tag{6}$$

and

$$R = r_1 r_2 \tag{7}$$

denote the transmittance and reflectance, respectively. Each surface has a coefficient (amplitude level) of reflection and transmission: r_1 and t_1 refer to the air:SiO_2 interface, and r_2 and t_2 refer to the SiO_2:Si interface. The last term in Eq. 5 is commonly called the Airy function, where

$$F = \frac{4R}{1-R^2}. \tag{8}$$

Finally, the transmission depends on the layer thickness, d, through the Airy function by

$$\Delta = \frac{4\pi n d}{\lambda}\cos\theta, \tag{9}$$

where θ is the angle of incidence of the beam with respect to the surface normal. Using n(SiO_2) = 1.5, and n(silicon) = 3.65, θ = 0 (a good approximation to laboratory conditions when the laser focus occurs at the device surface, and the beam wave-vector is normal to the surface), and the Fresnel equations [8], we find (see Fig. 3) that variations in layer thickness cause the transmission to vary over a range of ±16% about the median value. This variation should be compared to a variation of ±35% given in reference [5]. The results of the analysis given here have important ramifications for SEE measurements, since variations in the amount of charge needed to cause an upset should be due to variations in SEE immunity rather than to the amount of light reflected from the surface of a device. Typically, with good process control, the oxide thickness (around 1 μm)

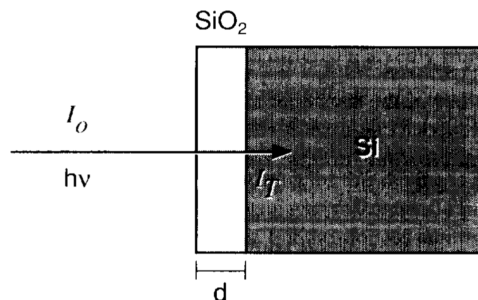

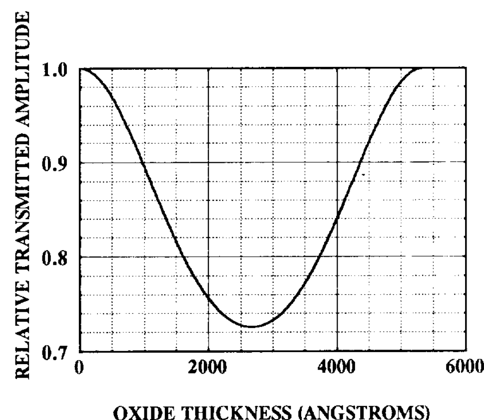

Figure 3. Above: diagram of device surface covered by a passivation layer of SiO_2. The effect of the passivation layer is to modulate the light intensity transmitted into the bulk silicon. The transmission depends on the thickness, d, of the layer, as well as on the refractive indices of SiO_2 and silicon. Below: relative transmittance of laser light into bulk silicon as a function of oxide thickness. The plot is obtained from the Airy term of Eq. 5 using the values for the refractive indices given in the text.

varies by < 10%, which implies that the maximum variation in transmission is < 7%. In a worst case scenario, where the passivation layer thickness varies by more than 1000 angstroms over the device area to be tested, it becomes necessary to measure the amount of light reflected from the surface for each spot that is tested. Thus, uncertainty in transmission due to passivation layer thickness may be eliminated.

We note that reflections from the back surface that may contribute to multiple upsets or add to the amount of charge generated in a particular junction should typically be of no concern because the light is diverging and the back surface is usually rough. Both of these factors contribute to the reduction of light intensity by orders of magnitude when the light reaches the junction near the front surface.

C. Nonlinear Absorption

It has been mentioned previously that, at high laser intensities, competing nonlinear absorption can seriously complicate the laser method [5]. That analysis was done for silicon, in the portion of the absorption spectrum (λ = 1.06 μm) very close to the bandgap. Working in this regime increases the possibility of significant nonlinear absorption because the relatively small value of the linear absorption coefficient requires that higher laser intensities be used to generate sufficient carrier densities to observe SEE effects. We argue below that because of increased nonlinear absorption, and other reasons related to the light-matter interaction, choosing a wavelength too near the bandgap is best avoided for device testing.

At high laser intensities used for testing circuits with high LET upset thresholds (typically 30-50 MeV-cm^2/mg) there is the possibility that additional higher order absorption mechanisms may modify the relationship between the light intensity and the carrier density. The most probable mechanism is due to the simultaneous absorption of two photons (TPA). In the presence of TPA the equation for light propagation may be written as

$$\frac{dI(z)}{dz} = -\alpha I(z) - \beta I^2(z) , \tag{10}$$

where $I(z)$ is the laser intensity propagating in the absorbing medium, and β is the two photon absorption coefficient (cm-s/Joule). The solution to Eq. 10 is found to be [9]

$$I(z) = I_o \frac{\exp(-\alpha z)}{1 + (\frac{\beta I_o}{\alpha})(1 - \exp(-\alpha z))} . \tag{11}$$

Here, I_o is the intensity entering the absorbing medium. The rate equation which determines carrier generation in the presence of both one and two photon absorption may be written as

$$\frac{dN(z)}{dt} = \frac{\alpha I(z)}{h\nu} + \frac{\beta I^2(z)}{2h\nu} , \tag{12}$$

where $N(z)$ is the carrier (electrons or holes) number density, $h\nu$ is the photon energy used in the experiment, and the factor of 2 in the case of TPA, takes into account the generation of one electron-hole pair for every two photons absorbed. Hence, there are two asymptotic limits. When TPA is negligible the number of carriers (EH pairs) may be equated with the number of photons. When TPA is dominant, the number of carriers is equal to half the number of photons contained in the laser pulse (this ignores light scattering processes, and other nonlinear optical effects that do not create carriers, but which are typically weak compared to absorption processes).

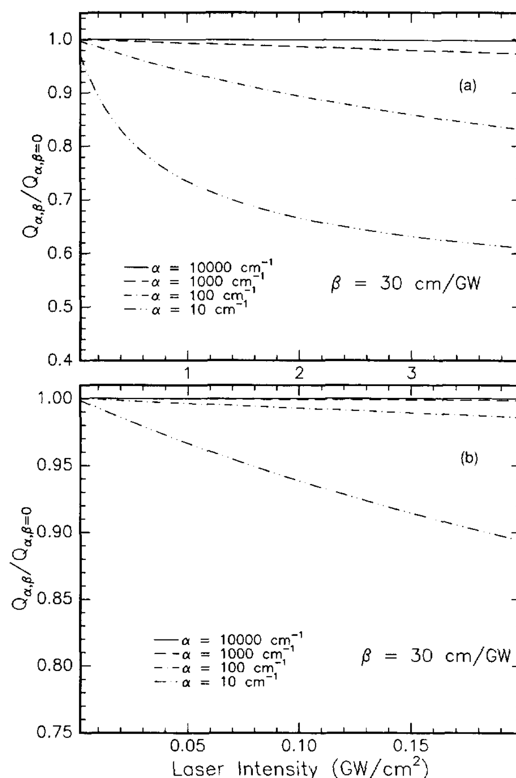

Figure 4. Charge generated in silicon by one- and two-photon absorption mechanisms as a function of laser intensity. The ordinate plots the ratio of charge generated by both one- and two-photon absorption to that of one-photon absorption alone ($Q_{\alpha,\beta}/Q_{\alpha,\beta=0}$). (a) Shows the dependence of charge generation on intensity up to 4 GW/cm^2, (b) shows intensity dependence on an expanded scale (up to 0.2 GW/cm^2). Each curve corresponds to a different choice of linear absorption coefficient α. A value of β = 30 cm/GW is chosen to approximate the two-photon absorption coefficient for each curve.

Case	Device Tested	Material	Pulsewidth (ps)	Wavelength (μm)	Pulse Energy Range Needed for Upset (pJ)	Intensity (MW/cm^2)	Maximum $\beta I_o/\alpha$
I [10]	Logic Circuit	GaAs	30	0.85	0.06-0.1	0.2-0.33	$8x10^{-7}$
II [11]	Logic Circuit	GaAs	2	0.62	0.05-1.5	2.5-75	$9x10^{-5}$
III [12]	SRAM	Silicon	15	0.652	21	62	$6.2x10^{-4}$
IV [2]	SRAM	Silicon	30	1.06	2-25	6.6-80	$2x10^{-1}$

Table 1. Range of upset thresholds for some silicon and GaAs devices measured by the pulsed laser method. Also shown are wavelength, laser pulsewidth, corresponding laser intensity, and the of the two-photon contribution (see. Eq. 11) for the largest measured upset threshold. The values for β are 23 cm/GW for GaAs, and 30 cm/GW for silicon.

Fig. 4 illustrates the effect of TPA on the amount of charge generated by a laser pulse. The graph models nonlinear absorption for silicon. A similar trend would be exhibited for GaAs. The graph plots the ratio of charge generated (electrons or holes) by both one- and two-photon mechanisms to that of just one photon absorption, or $Q_{\alpha,\beta}/Q_{\alpha,\beta=0}$, vs applied laser intensity. The charge is found by integrating Eq. 12 with respect to time and space co-ordinates. The ratio is plotted for several choices of linear absorption coefficient (α), and estimating β = 30 cm/GW for silicon [5]. The graph clearly shows that TPA effects become more pronounced as higher laser intensities are used, and as the ratio $\beta I_o/\alpha$ becomes larger (laser wavelength shifted closer to the bandgap for a given applied laser intensity). For example, for $\alpha = 10\ cm^{-1}$ (corresponding to $\lambda \sim 1.06$ μm for silicon; the YAG laser fundamental), a laser intensity of 1 GW/cm^2 yields a total generated charge that is $\approx$ 30% smaller than would be expected from linear absorption alone. [We note that the laser equivalent LET for silicon based on one photon absorption is ~ 5 $MeV\text{-}cm^2/mg$ for an applied intensity of 1 GW/cm^2; pulse energy = 100 pJ, pulsewidth = 10 ps, laser spot = $1\mu m^2$, and at λ = 1.06 μm] Clearly, when using intense laser pulses at a wavelength near the bandgap, any calculation of equivalent LET must take nonlinear absorption into account. By use of Eqs. (9,10) the effect of two-photon absorption can be included in the calculation of LET.

It must be stressed, however, that the majority of laser testing typically falls into a regime where the nonlinear contribution, $\beta I_o/\alpha$, is sufficiently small so that TPA may be ignored. Table 1 presents four cases [2,10-12] where the pulsed laser has been used to measure upset thresholds in devices. The table shows the range of laser intensities used to achieve the upsets, and the corresponding maximum value for the nonlinear contribution. In cases I and II, which correspond to testing of GaAs devices, the nonlinear contribution is quite negligible ($\beta I_o/\alpha$ is << 1). By using Fig. 4 as a rough guide (this graph was calculated using parameters for silicon), it is confirmed that the deviation from linear absorption is much less than 1% for these cases. For testing in silicon at 1.06 μm (case IV), Fig. 4 may be used directly. Here, even at the highest laser intensities needed to upset the hardest device, the deviation from linear absorption is predicted to be only $\approx$ 5%. In general, to observe appreciable TPA effects, the magnitude of the nonlinear term $\beta I_o/\alpha$ must be on the order of 1.

One advantage of the laser method is that the experimentalist has control over both the laser wavelength and the laser pulsewidth (which adjusts the laser intensity). These parameters may be adjusted to minimize TPA effects. For example, in the case of silicon, selecting a wavelength of 0.80 μm increases α to about 1000 cm^{-1}, so that the nonlinear contribution, $\beta I_o/\alpha$, is reduced by nearly a factor of 100 from its value at 1.06 μm (assuming the intensity is held constant). At λ = 0.80 μm in silicon, laser light would still have a $1/e$ penetration depth of $\approx$10 μm. Such a penetration depth is sufficient for testing modern devices built on epilayers (typically, with a thickness on the order of 10 μm), since charge deposited in the highly doped substrate is not efficiently collected. Finally, typical testing conditions for devices fabricated from GaAs results in $\beta I_o/\alpha < 10^{-4}$ (unless λ is close to the bandgap), which further reduces the effect of TPA.

Fig. 5 presents an experimental confirmation that TPA may be ignored for typical laboratory testing conditions. Here, the device is a GaAs HIGFET, which is irradiated by λ = 0.62μm laser pulses with the beam focused to a 1 μm spot. The laser pulse energy, and therefore the number of photons, in each case is kept constant, but the intensity is changed by adjusting the laser pulsewidth over a range of 1.5 - 15 ps. The corresponding change in intensity varies the two-photon

contribution by two orders of magnitude. The data, which show a constant charge collected at each applied laser intensity (within experimental error), confirm that TPA is not a factor under these conditions.

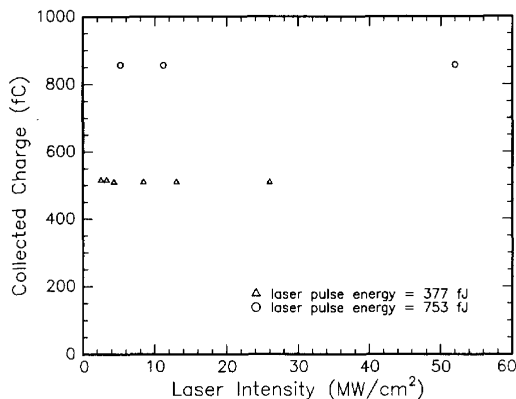

Figure 5. Experimental charge collection in a GaAs HIGFET as a function of applied laser intensity. The laser intensity is controlled by changing the pulsewidth gradually from 1.5 to 15 ps. The pulse energy (hence, the number of photons) for each choice of applied laser intensity is held constant. Irradiation occurs in a 1 μm spot.

D. Choice of Optical Wavelength

Previous analysis of the laser technique has suggested that a working wavelength of 1.06 μm for testing silicon devices is an optimum choice because of the deep penetration depth (700 μm) [5]. Many of the subsequent criticisms of the laser technique were then made based upon this choice of wavelength [5]. In the following section we argue that such a choice of optical wavelength is not, in general, an optimum choice, and that the criticisms of the laser technique based upon selection of λ = 1.06 μm are, *at the least*, less significant when wavelengths farther above the bandgap are used. For investigating SEE in silicon devices, we argue that a working wavelength around λ = 0.80 μm is a more optimum choice.

E. Bandgap Narrowing

The energy bandgap depends on the carrier density through two effects - bandgap renormalization and the Burstein-Moss shift. High doping levels reduce the bandgap through bandgap renormalization, whereas the Burstein-Moss shift increases the effective bandgap because carriers at the bottom of the conduction band in n-type material fill up states that are then not available for electron transitions from the valence band [13]. In silicon, the net effect of bandgap renormalization and the Burstein-Moss shift is to reduce the bandgap, and, thus, increase absorption as the carrier density increases. Fig. 6 shows the effect of bandgap narrowing in silicon [5]. At λ = 1.06 μm (1.17 eV) one sees that the absorption coefficient changes significantly as the doping level increases. The effect on GaAs (not reproduced here) is even more pronounced at the bandgap. Thus, for devices that contain layers with varying degrees of doping, it becomes difficult to accurately predict the amount of charge generated when using laser wavelengths which are close to the bandgap. However, by selecting a wavelength that is farther above the bandgap, it is seen from Fig. 6 that the absorption coefficient becomes much less sensitive to doping density. For silicon, a much better working wavelength is between 0.80-0.85 μm (1.45-1.55 eV), which is easily generated with conventional dye lasers, or with newer titanium sapphire laser technology. In this region, the sensitivity to absorption coefficient is minimized while still preserving a relatively deep penetration distance (10-20 μm). In GaAs devices, because of the relatively steep absorption curve, it is not possible to choose a wavelength that minimizes absorption coefficient sensitivity to doping density while preserving a relatively long penetration distance. Yet, it is worth pointing out that recent experimental work [4] and computer modeling [14] of charge collection in devices suggest that, even when the light penetration is confined to the surface region of the device (≤1 μm), the charge collection dynamics initiated by both laser light and by the ion appear to be quite similar.

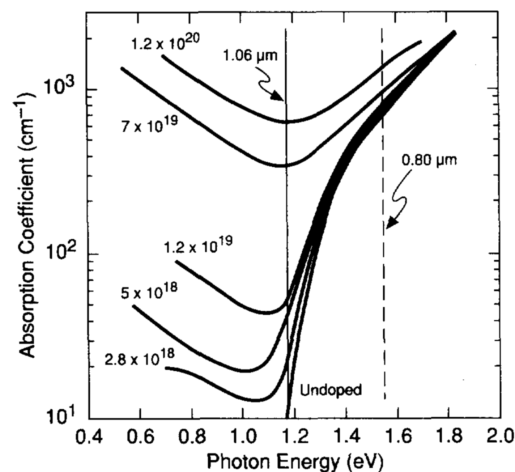

Figure 6. Absorption coefficient for silicon at various doping levels of p-type material [After A.H. Johnston, IEEE Trans. Nuc. Sci. NS-40, 1694 (1993)]. The solid line and dashed line indicate the photon energies corresponding to λ = 1.06 μm and λ = 0.80 μm, respectively.

F. Free Carrier Absorption

At very high carrier density, light may be absorbed efficiently by free carriers. This effect is important only when the plasma frequency is comparable the frequency of light (10^{15} s^{-1}). The formula for the plasma frequency is [13]

$$\omega_p^2 = \frac{Ne^2}{m^* \varepsilon_o \varepsilon_r}, \tag{13}$$

where N is the carrier density, m^* is the carrier effective mass, e is the electron charge, ε_o is the permittivity of free space, and ε_r is the dielectric constant. Considering the case of silicon, a carrier density of 10^{19}/cm^3, an effective mass of 0.15 m_o, and a dielectric constant of 10, yields a plasma frequency of ~ 10^{14} s^{-1} (or a plasma wavelength of ~ 3.3 μm). This is below that of typical laser frequencies used in device testing (3-5×10^{14} s^{-1}), and, thus, free carrier absorption may be ignored.

Free carrier absorption may also occur by carriers generated by laser light, i.e., the leading edge of the laser pulse, if sufficiently intense, can generate carriers which then absorb an appreciable fraction of the trailing edge of the pulse. To make an accurate estimate, an analysis of the coupled equations governing pulse propagation and quantum absorption is necessary, and is beyond the scope of this paper.

III. LASER VS ION CHARGE COLLECTION

From the analysis given above, both material absorption and beam spreading leads to an initial laser track with a significantly lower charge density than that initially produced by an ion. This is a central difference between the two techniques, and may affect the amount of charge collected. In this section, we discuss the effects of funneling and Auger recombination since they each depend on charge density, and, thus, may significantly affect charge collection following ion or laser excitation.

A. Funneling

When a charge track with a density greater than the doping density of the semiconductor passes through a junction, the electric field associated with the junction is distorted, producing a funnel that gives rise to additional charge collection [15]. The track density determines the length of the 'funnel' which, in turn, determines the amount of charge collected in excess of that deposited in the depletion region. By showing experimentally that the amount of charge collected across a diode junction irradiated with a laser pulse depends on the total beam energy to the 4/3 power, it was confirmed that funneling plays a role in charge collection for both ions and laser light [1]. However, to see the power dependence in devices with high doping levels using the relatively wide laser beam, it was necessary to use very high laser energies to generate sufficient charge to exceed the background charge density. In cases where funneling contributes a significant amount of charge to ion-induced upsets, larger equivalent LETs will be needed for the laser. This is one reason why the laser cannot replace the accelerator for determining *absolute* values for SEE thresholds.

B. Carrier Lifetime

There are several factors which influence the carrier lifetime, and at the high carrier density generated in an ion track, or with an intense laser pulse, it is expected that Auger recombination becomes significant. Auger recombination occurs when free electrons in the track collide, resulting in one electron losing energy to another. For high injected carrier densities, the recombination time may be written as [16]:

$$\tau = \left(\frac{3n_i^2}{\Delta n^2}\right)\tau_i \tag{14}$$

where n_i is the intrinsic carrier concentration, Δn is the injected carrier density, and $\tau_i = 4.48\times10^9$ sec is the intrinsic Auger lifetime in silicon [16].

At high carrier densities the recombination time becomes very short, limiting the amount of collected charge. For carrier densities approaching 10^{21}/cm^3 the Auger lifetime in silicon is on the order of a picosecond. The Auger recombination time is much shorter in an ion-generated track than in the much lower density track produced by the laser, and, therefore, of much greater importance. Thus, more charge is lost via Auger recombination in the ion track than in the laser track. Charge lost via Auger recombination has been observed experimentally for heavy ion fission products in surface barrier detectors [17].

An important point still not fully understood is the degree to which recombination and funneling cancel each other out. A partial cancellation could reduce the difference in the amount of charge collected by ions and laser light arising from differences in track charge density, and, in some cases, the threshold LETs measured by the two techniques may not be significantly different. In general, it is not true (as implied in ref. 5) that correlating laser measurements with ion measurements depends solely on the existence of funneling. Further theoretical work is needed in order to quantify the extent to which both funneling and recombination effects modify charge collection in the laser and ion methods.

IV. EXPERIMENTAL AND THEORETICAL COMPARISON OF LASER AND ION INDUCED CHARGE COLLECTION

The previous sections emphasized the difference in charge tracks generated by laser light and by ion strikes, and how this may lead to different amounts of charge collected, and ultimately, to different results for SEE measurements. In

this section we present experimental data and theoretical simulations which suggest that, despite the very different charge tracks generated by the laser and ion techniques, there remains a remarkable similarity in the characteristics of laser and ion generated charge collection. This evidence supports the feasibility of employing laser-based testing for SEE phenomena.

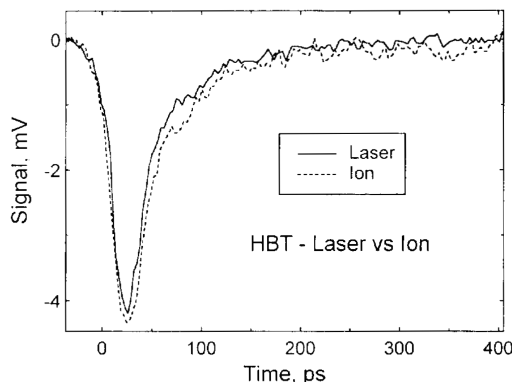

Figure 7. Comparison of charge collection transients for laser and ion 3-MeV alpha particle excitation of a GaAs HBT. The laser power was adjusted so that the amplitude of the laser generated transient matched that of the ion. The bias conditions for the two curves are the same.

There have been several recent experimental studies which have demonstrated that above bandgap laser pulses provide an invaluable tool for investigating the mechanisms of charge collection dynamics [4], and for practical measurements of SEE phenomena [1-3,11,18]. In Fig. 7, we reproduce data which compare the charge collection transients produced by picosecond laser pulses ($\approx$ 2 ps) and 3-MeV alpha particles for the GaAs HBT devices [4]. Here, the applied laser intensity (corresponding to a 19 fJ laser pulse) was adjusted so that the amplitude of the laser generated transient matched that of the ion. The data clearly convey that the laser and ion transients are nearly indistinguishable, at least for the time resolution provided by the experiment, which is about 10 ps. More significant differences in the two transients are expected to occur on a timescale of $\leq$1 ps, where processes such as funneling and Auger recombination are significant due to higher initial charge density. Recently, we observed a comparable similarity in laser and ion transients in a GaAs HIGFET device [19]. This is a significant result since charge transport is quite different in these two devices due to their different construction. Computer simulations for laser and ion generated charge collection provide additional confirmation

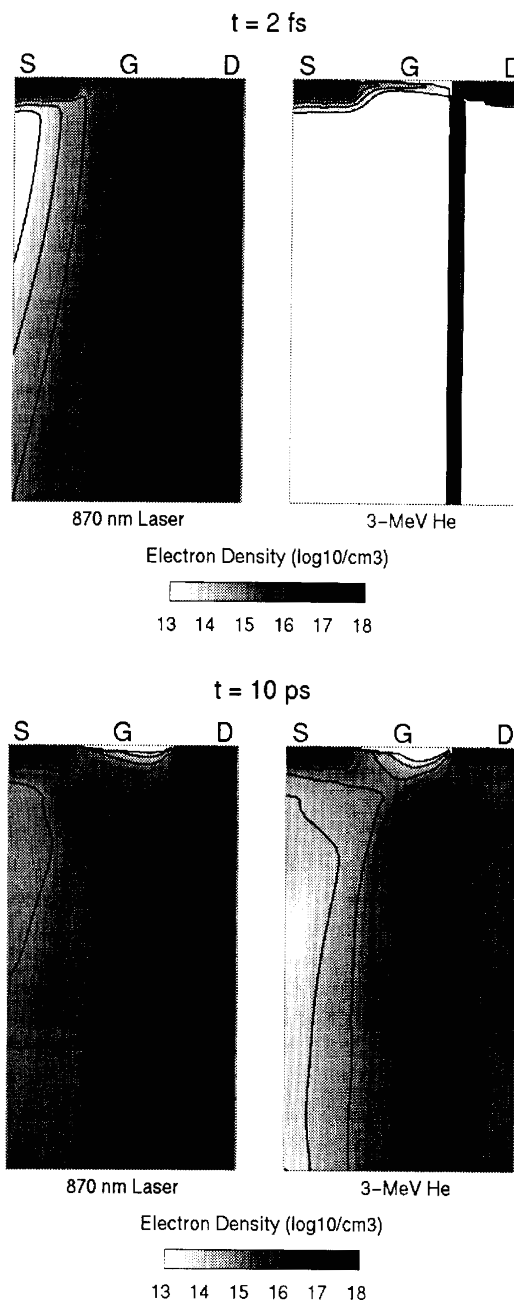

Figure 8. Two-dimensional computer simulations of charge collected in a model GaAs MESFET. Top: electron density at 2 fs after laser excitation (left) and 3-MeV alpha particle strike (right). Bottom: corresponding electron density after 10 ps. The 1/e penetration depth of the laser is 8.5 μm. The depth of the model MESFET is 4 μm. The laser pulse and alpha particle each initially deposit about 25 fC in the area shown. V_{gs} = 0 V, V_{ds} = 2.0 V.

of the qualitative similarity in the charge collection mechanism for ions and laser pulses. Figure 8 presents an example of a 2-D simulation of charge collection dynamics for both laser and ion excited GaAs MESFETs. In this example the laser excitation is at 0.87 μm (1/e depth ≈ 8 μm), and 3-MeV alpha particles are used for ion excitation. The graph shows the electron distribution at 10 ps after excitation by both laser and ion. The laser excitation generates a charge distribution that is 1 μm in diameter at the surface, while the ion generates a charge track that is much narrower, ≈ 0.02 μm. Despite the large initial difference in track structure, the calculation shows how the charge distributions have evolved on an ultrafast timescale (< 10ps!) to a state where they have become qualitatively similar. This result provides theoretical support to the experimental observations that show qualitative similarity in laser and ion charge collection transients.

V. PULSED LASER SEE APPLICATIONS AND LASER/ION SEE FEASIBILITY COMPARISON

Despite the differences in the laser and ion techniques mentioned above, there remains a strong enough similarity in the ion-semiconductor and photon-semiconductor interaction to permit extensive application of the pulsed laser to SEE testing. In this section, we outline some of the important SEE applications for which the pulsed laser is well suited. We also make a feasibility comparison of the laser and ion techniques towards several SEE applications, which is based upon previously published work, as well as work currently in progress. We begin by illustrating several advantages the pulsed laser offers to SEE testing:

1. Spatial Information. The laser can be focused down and imaged to a small spot (≤1 μm). Thus, the sensitivities of individual transistors within the circuit can be measured [18]. This is not easily accomplished with the ion technique [20,21].

2. Temporal Information. The laser may be easily synchronized to the circuit clock so that SEE measurements may be performed as a function of timing. Recent work [18] has shown how upsets in logic circuits are sensitive to the arrival of a laser pulse with respect to the circuit clock. To our knowedge, similar information has not been obtained with an accelerator.

3. Nondestructive. As long as the laser intensity is below that which produces melting in the semiconductor there is no permanent damage to the material. In contrast, ion testing causes damage to the circuit that is dependent on total dose. This not only limits the life of the circuit, but, also, may affect the results of the measurements.

4. Relative LET Threshold. As mentioned above the relative SEE threshold of a circuit may be easily determined by adjusting the laser intensity.

5. Convenience. The laser technique is convenient because it is totally compatible with a fabrication facility. There is no ionizing radiation threat, and the entire system can be enclosed in a light-tight box to avoid the possibility of eye damage. No vacuum is required for testing, the LET can be varied by merely changing the light intensity, and setup time is very short.

6. Cost. Laser testing is relatively inexpensive. For example, a complete laser testing system can currently be purchased for about $150K. As laser technology continues to advance it is anticipated that the cost of laser testing will further decrease.

The laser technique is not without its own limitations. They include:

1. No Absolute Measure of SEE Threshold. Since light and ions do not interact in the same way with the semiconductor, they produce different initial track structures. These are expected to manifest themselves in differences in measured LET upset thresholds.

2. No Direct Measure of the Asymptotic Cross-Section. To calculate error rates, the variation of the cross-section with LET must be measured. Using only the threshold LET and the limiting cross section may overestimate the error rate by up to an order of magnitude. The laser can be used to estimate the limiting cross section indirectly by identifying which nodes are sensitive to upset and then using the circuit layout to add up all the sensitive areas.

3. Inability of Light to Penetrate Metal. An ion will pass through metal but a laser pulse will not. When testing some devices this is a problem. For example, the 93L422 256x4 bipolar SRAM has an upset threshold that varies across the surface of the sensitive volume. If the most sensitive region is covered by metal, then the laser will be unable to measure the threshold. The problem is exacerbated in devices where the sensitive nodes are completely covered by metal. As more and more transistors are incorporated on a single chip, greater use will be made of multilevel interconnects that cover SEE-sensitive areas. This may limit the usefulness of the laser technique with regard to measuring upset threshold. However, to date many circuits have been successfully probed.

A central point that deserves emphasis is that many SEE applications do not require that the laser and ion methods give the same LET upset threshold. One such application for which the laser is uniquely suited to is hardness assurance. SEE hardness assurance involves measuring either every circuit, or at least a representative number of circuits or test structures to ascertain whether they meet SEE specifications. At present, if done at all, hardness assurance is only carried out on a few representative circuits at an accelerator facility using ions that produce a small but finite amount of damage to the circuit. The availability of a nondestructive,

convenient, inexpensive, and rapid test for hardness assurance is an attractive prospect because it would make possible the testing of a large number of circuits. The pulsed laser adequately satisfies all of these requirements. For hardness assurance testing it is *not* necessary that the laser and ion give the same LET upset thresholds provided 1) the relative numbers agree, and 2) there exists a fiduciary set of measurements for that type of circuit comparing ion and laser upset thresholds. When testing a circuit for SEE sensitivity with both an ion and pulsed laser, the laser threshold can be compared directly to an ion threshold. All subsequent measurements can then be done with the laser. Any variations in SEE threshold can be referred to the ion data for absolute values, provided the variations are not unique to the laser measurements.

Application	Laser	Ion	Comments/References
Timing Effects	Yes	No	Laser: [2], [4], [18] Not easily performed with ion
Spatial Effects	Yes	Yes	Laser: [2] Ion: [20], [21] Ion measurements difficult
Hardness Assurance	Yes	No	Laser: [2] Ion technique not practical
Bit Maps	Yes	No	Laser: [22] Ion technique not practical
Fault Tolerance	Yes	Limited	Laser: [22]
Fundamental Studies	Yes	Yes	Laser: [4] Ion: [23], [24] Radiation damage limits ions
SEU Threshold	Yes	Yes	Laser: [2] Laser thresholds should be calibrated
σ vs Effective LET	No	Yes	
σ Saturation	Indirect	Yes	Ion: [25]
Software Validation	Yes	No	Laser: [22]
Detailed Circuit Evaluation	Yes	No	Laser: [22]

Table 2. Laser/ion feasibility comparison for several SEE applications.

Given the emergence of pulsed laser as an alternative technique for SEE testing, it is useful at this stage to make a feasibility comparison between laser and ion methods. Table 2 lists a range of device testing applications where either ion or laser methods (or both) have been used to characterize SEE-related phenomena. While the list is not exhaustive, it certainly includes many of the applications of current interest to the SEE community. For each application, the laser and ion methods are rated based on feasibility considerations - i.e., whether or not the method may be implemented in a relatively simple and practical way - as opposed to whether "in principle" either method may be applied. Where possible, reference is made to past work. The table shows that for a variety of SEE applications the pulse laser offers a sensible alternative to ion testing, and, in some cases is the clear choice.

VI. CONCLUSIONS

We have presented an analysis of the pulsed picosecond laser as a technique to explore SEE events in modern semiconductor devices. We have commented on previous criticisms of the laser technique [5] which were based largely on what was perceived to be the experimentalist's inability to account for various optical uncertainties and nonlinearities in the degree of laser induced charge generation. Our conclusion is that differences between laser and ion generated charge that result from purely optical effects (e.g., laser beam propagation, laser wavelength, linear and nonlinear absorption, reflection and interference effects) do not necessarily impose serious limitations on the laser technique. Each effect can be taken into account by use of well known optical expressions, or minimized by careful experimental practice. Most important is that proper implementation of the laser technique rests upon a judicious choice of the working wavelength. As shown above, the working wavelength can be chosen in a way to minimize uncertainties in absorption due to changing doping densities in different regions of the device, while maintaining a deep enough penetration distance so that the laser excitation represents a reasonable approximation to ion excitation.

More significant for SEE measurements is the difference in charge tracks generated by laser and ions, which, because of effects such as funneling and Auger recombination, may lead to different amounts of charge collected, and, hence, different values for SEE quantities such as upset threshold. While preliminary work has suggested there is a large degree of similarity in charge collection from tracks initiated by lasers and ions, additional experimental and theoretical work will be needed to better understand the role played by charge collection and transport mechanisms, and their relative importance in both laser and ion SEE measurements.

We close by emphasizing that there are both advantages and limitations to the pulsed laser technique. On balance, however, the pulsed laser is an extremely powerful and useful technique for SEE testing. In our view, the laser technique will not replace ion testing, but will, at the least, be a complimentary technique that will provide invaluable information in characterizing SEE in circuits.

VII. REFERENCES

[1] S. Buchner, A.R. Knudson, K. Kang, and A.B. Campbell, "Charge Collection from Focussed Picosecond Laser Pulses", IEEE Trans. Nuc. Sci. NS-35, 1517 (1988).

[2] S. Buchner, K. Kang, W.J. Stapor, A.B. Campbell, A.R. Knudson, P. McDonald, and S. Rivet, "Pulsed Laser-Induced SEU in Integrated Circuits: A Practical Method for Hardness Assurance Testing", IEEE Trans. Nuc. Sci. NS-37, 1825 (1990).

[3] S. Buchner, W.J. Stapor, J. Langworthy, and A.B. Campbell, "Implications of the Spatial Dependence of the Upset Threshold of the 93L422 SRAM Measured with a Pulsed Laser", IEEE Trans. Nuc. Sci. NS-41, (December 1994).

[4] D. McMorrow, J.S. Melinger, A.R. Knudson, T.R. Weatherford, A.B. Campbell, and W. Curtice, "Picosecond Charge Collection Dynamics in GaAs MESFETs", IEEE Trans. Nuc. Sci., NS-39 (1992); D. McMorrow, T R. Weatherford, A.R. Knudson, L.H. Tran, J.S. Melinger, and A.B. Campbell, "Single-Event Dynamics of High-Performance HBTs and MESFETs", IEEE Trans. Nuc. Sci. NS-40, 1858 (1993).

[5] A.H. Johnston, "Charge Generation and Collection in p-n Junctions From a Pulsed Infrared Laser", IEEE Trans. Nuc. Sci., NS-40, 1694 (1993).

[6] A. Yariv, *Quantum Electronics*, John Wiley and Sons, New York 1975.

[7] W.J. Stapor, and P. McDonald, "Practical Approach for Ion Track Energy Distribution," J. Appl. Phys. , 64, 4430 (1989).

[8] G. Fowles, *Introduction to Modern Optics*, Holt-Rinehart-Winston, 1975.

[9] E.W. Van Stryland, H. Vanherzeele, M.A. Woodall, M.J. Soileau, A.L. Smirl, S. Guha, and T.F. Bogess, "Two-Photon Absorption, Nonlinear Refraction, and Optical Limiting in Semiconductors," Opt. Eng., 24, 613 (1985).

[10] R. Schneiderwald, D. Krening, S. Buchner, K. Kang, and T.R. Weatherford, "Laser Confirmation of SEU Experiments in GaAs MESFET Combinational Logic," IEEE Trans. Nuc. Sci. NS-39, 1665 (1992).

[11] D. Fouts, T.R. Weatherford, D. McMorrow, J.S. Melinger, and A.B. Campbell, "Single Event Upset in GaAs Dynamic Logic," IEEE Trans. Nuc. Sci. NS-41, (December 1994)

[12] Q. Kim, H. Schwartz, K. McCarty, J. Cross, and C. Barnes, IEEE Radiation Effects Data Workshop, July 21, 1993, Snowbird UT, pgs. 99-106.

[13] J. Pankove, *Optical Processes in Semiconductors*, Prentice-Hall, New Jersey, (1971).

[14] T.R. Weatherford, D. McMorrow, W.R. Curtice, A.R. Knudson, and A.B. Campbell, "Single Event Induced Charge Transport Modeling in GaAs MESFETs," IEEE Trans. Nuc. Sci. NS-40, 1867 (1993).

[15] C.M. Hsieh, P.C. Murley, and R.O. O'Brien, "A Field Funneling Effect on the Collection of Alpha-Particle Generated Carriers in Silicon Devices," IEEE Elect. Device Lett., EDL-2, p. 102 (1981).

[16] S.S. Li, *Semiconductor Physical Electronics*, Plenum, New York (1993).

[17] E.C. Finch, M. Ashgar, and M. Forte, "Plasma and Recombination Effects in the Fission Fragment Pulse Height Defect in a Surface Barrier Detector," Nucl. Instrum. and Methods," **163**, 467 (1979).

[18] S. Buchner, K. Kang, W.J. Stapor, and S. Rivet, "Spatial and Temporal Dependence of Single Event Upsets in a 64K SRAM Using a Pulsed Laser," IEEE Trans. Nucl. Sci. NS-39, 1630 (1992).

[19] D. McMorrow, J.S. Melinger, N. Thantu, A.B. Campbell, T.R. Weatherford, A.R. Knudson, L.H. Tran, and A. Peczalski, "Charge Collection Mechanisms of Heterostructure FETs," IEEE Trans. Nuc. Sci. NS-41, (December 1994)

[20] F.W. Sexton, K.M. Horn, B.L. Doyle, J.S. Laird, M. Cholewa, A. Saint, and G.J.F. Legge, "Relationship Between IBICC Imaging and SEU in CMOS ICs," IEEE Trans. Nuc. Sci. NS-40, 1787 (1993).

[21] A. Campbell, A. Knudson, D. McMorrow, W. Anderson, J. Roussos, S. Espy, S. Buchner, K. Kang, D. Kerns, and S. Kerns, "Ion Induced Charge Collection in GaAs MESFETs," IEEE Trans. Nuc. Sci. NS-36, 2292 (1989).

[22] S. Buchner, (Unpublished Results).

[23] B.W. Hughlock, G.S. Larue, and A.H. Johnston, "Single Event Upset in GaAs E/D MESFET Logic," IEEE Trans. Nuc. Sci. NS-77, 1894 (1990).

[24] B.W. Hughlock, T. Williams, A. Johnston, R. Plaag, "Ion Induced Charge Collection in GaAs MESFETs and its Effect on SEU Vulnerability," IEEE Trans. Nuc. Sci. NS-38, 1442 (1991).

[25] R. Koga, S.D. Pinkerton, S.C. Moss, D.C. Mayer, and S. LaLumondiere, "Observation of Single Event Upsets in Analog Circuits," IEEE Trans Nuc. Sci., NS-40, 1838 (1993).